

**NASA TECHNICAL
MEMORANDUM**



NASA TM X-1582

NASA TM X-1582

GPO PRICE \$ _____

CFSTI PRICE(S) \$ _____

Hard copy (HC) _____

Microfiche (MF) _____

692 July 68

FACILITY FORM 102	ACCESSION NUMBER	THRU
	PAGES	CODE
	NASA CR OR TMX OR AD NUMBER	CATEGORY

**EFFECTS OF HIGH-WAVE
AMPLITUDE AND MEAN FLOW
ON A HELMHOLTZ RESONATOR**

by Bert Phillips

Lewis Research Center

Cleveland, Ohio



EFFECTS OF HIGH-WAVE AMPLITUDE AND MEAN FLOW
ON A HELMHOLTZ RESONATOR

By Bert Phillips

Lewis Research Center
Cleveland, Ohio

NATIONAL AERONAUTICS AND SPACE ADMINISTRATION

For sale by the Clearinghouse for Federal Scientific and Technical Information
Springfield, Virginia 22151 - CFSTI price \$3.00

ABSTRACT

An experimental investigation was conducted to determine the effects of mean flow and high-wave amplitude on the impedance of a Helmholtz resonator. The oscillatory phase and pressure relations across the aperture of a resonator were measured and converted into values of acoustic resistance and reactance. The results indicate that (1) the aperture effective length in a rocket-engine environment should be considered approximately equal to the aperture thickness and (2) the acoustic resistance at high-wave amplitude can be considered to be a turbulent jet loss.

STAR Category 12

EFFECTS OF HIGH-WAVE AMPLITUDE AND MEAN FLOW ON A HELMHOLTZ RESONATOR

by Bert Phillips

Lewis Research Center

SUMMARY

An experimental investigation was conducted at the Lewis Research Center to determine the effects of mean flow and high-wave amplitude on the impedance of a Helmholtz resonator. Data were obtained by flush mounting a Helmholtz resonator in the wall of a wind tunnel equipped with acoustic drivers. The oscillatory phase and pressure relations across the aperture were measured and converted into values of acoustic resistance and reactance. The results indicate that (1) in the rocket-engine environment, the aperture effective length should be considered approximately equal to the aperture thickness and (2) the acoustic resistance at high-wave amplitude can be considered a turbulent-jet loss defined by the product of the gas density and particle velocity.

INTRODUCTION

Extensive testing at the Lewis Research Center and elsewhere has shown that an array of Helmholtz resonators can damp combustion instability in rocket-combustion chambers (refs. 1 and 2). These arrays or liners were designed by using a set of equations to calculate α , the normal acoustic absorption coefficient. The equations for calculating α were both theoretical and empirical. Effective application of the equations to the design of a rocket-engine liner depend on a knowledge of gas properties in the resonator cavity, the effects of mean flow past and through the resonator apertures, and the effects of high-wave amplitude on the resonator impedance. With these defined, α can be readily calculated from the resonator impedance.

The effects of high-wave amplitude on the real part of the resonator impedance (resistance) are presented in references 2 to 4; however, the results differ widely. Also presented in reference 3 are data on the effect of high-wave amplitude on the resonator inductance, but this effect was negligible and not included in the design equations of ref-

erence 2. Wave-amplitude effects were measured with an impedance tube in references 2 to 5. The extreme sensitivity of this apparatus may account for the difference in experimental results reported.

The effects of mean flow past the resonator apertures are presented in references 6 and 7, and the effects of mean flow past and through the apertures are presented in reference 8. The results of reference 7 were obtained with a lined duct, whereas those of reference 8 were obtained with a modified impedance tube. Comparison of the results of references 7 and 8 for the effect of mean flow past the apertures on the inductance and the resistance shows marked disagreement. In addition, the correlation of the effects of mean flow past the aperture on resistance, taken from reference 6 and used in the design equation of reference 2, may not be valid because it was obtained from results with woven porous plate rather than perforated plate.

The objectives of this investigation were (1) to evaluate an improved experimental method that can determine the effects on resonator impedance of both mean flow past the resonator aperture and high-wave amplitude, (2) to study the effects of mean flow past the resonator aperture and high-wave amplitude on the resistance and the inductance of several resonator configurations, and (3) to resolve some of the conflicting results existing in the reference material.

The experimental method involved mounting a single Helmholtz resonator within a subsonic wind tunnel. The tunnel flow field was acoustically excited by an electrical or siren driver, both with and without flow past the resonator aperture. By measuring the phase and amplitude relations of the oscillatory pressure across the resonator aperture, the resistance and the inductance were immediately determined. The advantages of this method over those used previously are (1) that the mean flow is past the external face of the resonator, similar to conditions in a rocket engine, (2) that it is relatively insensitive to small errors in the measurement of sound pressure levels and positions, and (3) that both high-wave amplitude and flow could be simultaneously evaluated in this apparatus.

The scope of the investigation is indicated by the following table:

Resonator aperture diameter, in.; cm	0.375; 0.95
Resonator neck lengths, in.; cm	0.1875, 0.375; 0.475, 0.95
Resonator depths, in.; cm	0.9 to 2.3; 2.28 to 5.85
Frequencies, Hz	700 to 1300
Sound amplitudes, dB	120 to 163
Maximum flow velocities, ft/sec; m/sec.	0 to 360; 0 to 109.8

APPARATUS

Wind Tunnel

The apparatus for determining flow effects was the same as described in reference 6 and is shown in figures 1 and 2. The cylindrical test section is 10.85 inches (27.5 cm), inside diameter, with an overall length of 18 inches (45.7 cm). The ends of the test section are faired into a wind tunnel with rubber walls to minimize structure-transmitted noise. The flow profile and magnitude were measured at position A-A in figure 2 by a pitot-static probe. In all tests, the flow was dry air at ambient temperature.

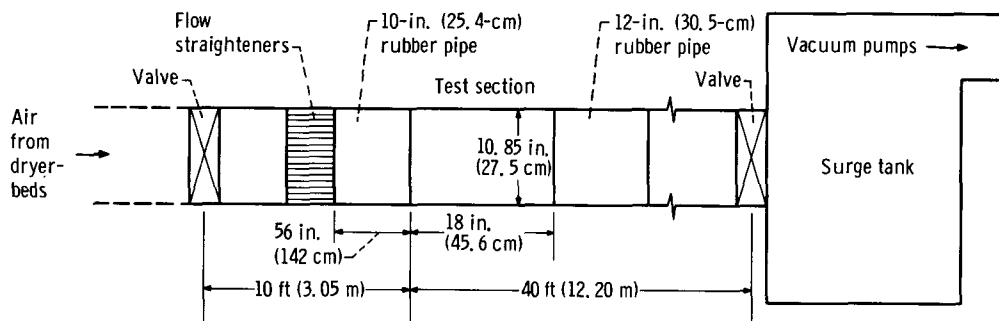
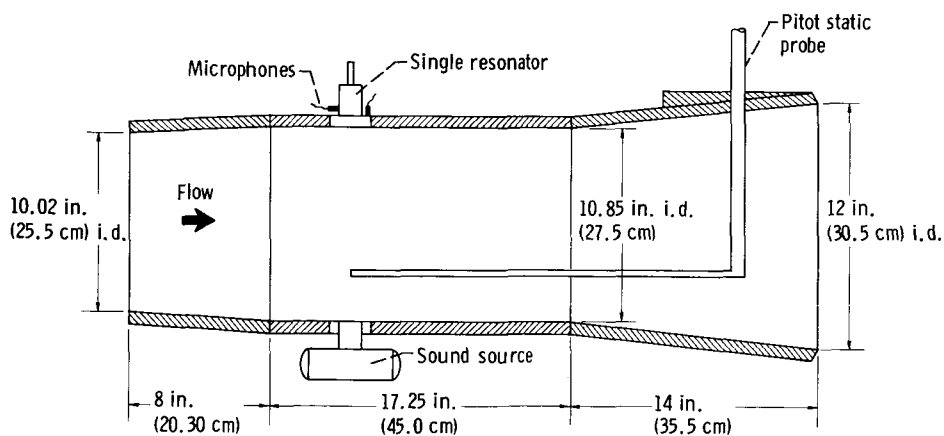


Figure 1. - Tunnel test system.



CD-9651

Figure 2. - Tunnel test section.

Single Resonator

A sectional view of the single resonator tested is presented in figure 3. The variable-depth plunger was moved manually.

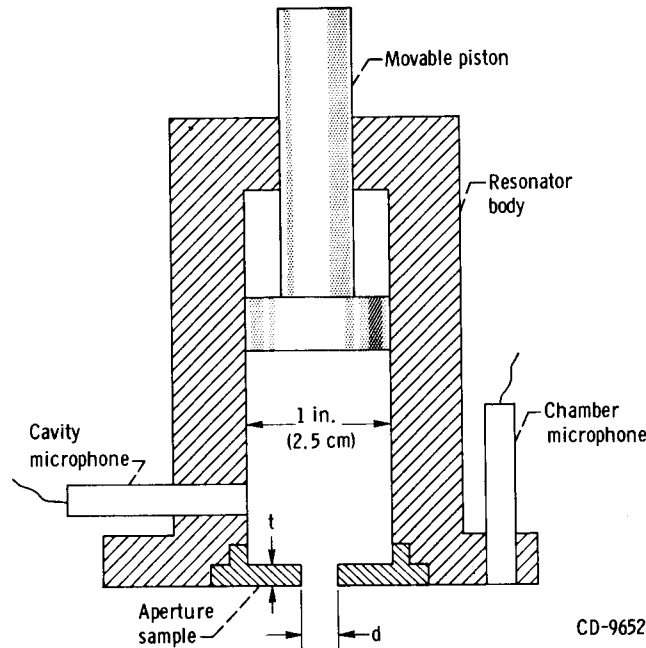


Figure 3. - Single resonator cross section.

Acoustic Source

The acoustic field was produced by an electrical or siren driver. The electrical power for the driver was an audio-oscillator amplified to a power level between 30 to 100 watts. The pneumatic input for the siren driver was 300 standard cubic feet per minute ($7.5 \text{ m}^3/\text{min}$) of dry air at 40 psig (275 kN/m^2 gage). (A maximum amplitude of 163 dB opposite the resonator aperture was possible.) The siren flow was diverted in order to prevent impingement on the resonator.

Measuring Instrumentation

The instrumentation consisted of two high-impedance, 1/4-inch (0.635-cm) microphones which had a flat response to approximately 5000 hertz, a phase meter accurate

to 2° and an rms sound level meter accurate to 1 decibel connected in parallel.

PROCEDURE

Nonflow Testing

The single resonator was mounted on the test chamber. The plunger was positioned to give minimum volume in the cavity. The driver was switched on and the audio-oscillator (driver) amplitude adjusted to give the maximum amplitude at microphone 2 (see fig. 3) for each test in the frequency range (700 to 1300 Hz). The plunger was then moved, with the phase and amplitude relations between microphones 1 and 2 recorded against plunger position (i. e. , cavity volume).

Flow Testing

A series of flow velocities at the centerline of the test section was established by throttling upstream and downstream valves. At each flow, the procedure then became identical to that for nonflow.

THEORY

Considering a Helmholtz resonator as a lumped parameter system, the following expression for its operation can be obtained:

$$\left. \begin{aligned} 2P_i \cos \omega t &= R_m \dot{x} + M\ddot{x} + Cx \\ \text{Impedance} &= R_m + i\left(\omega M - \frac{C}{\omega}\right) \end{aligned} \right\} \quad (1)$$

where

P_i incident wave (zero to peak) pressure, lb/ft²; N/m²

ω angular wave frequency, rad/sec

τ time, sec

R_m resistance, (lb force)(sec)/ft³; (N)(sec)/m³

M inductance, (lb force)(sec²)/ft³; (N)(sec²)/m³

- C capacitance, (lb force)/ft³; N/m³
 x displacement of gas slug in neck of resonator, ft; m
 M - (C/ω) reactance

The solution is

$$x = \frac{2P_i \sin(\omega\tau - \varphi)}{\omega \sqrt{R_m^2 + \left(\omega M - \frac{C}{\omega}\right)^2}} \quad (2)$$

where

φ phase angle between particle velocity and pressure equal to $\arctan \frac{\left(\omega M - \frac{C}{\omega}\right)}{R_m}$

Based on the gas dynamics of the resonator, the following definitions are given:

$$R_m = R + \frac{2\rho c S}{g\lambda^2} \quad (3)$$

(from ref. 9) where

- R acoustic resistance, (lb force)(sec)/ft³; (N)(sec)/m³
 λ wavelength, ft; m
 ρ density, (lb mass)/ft³; kg/m³
 c sonic velocity, ft/sec; m/sec
 g gravitational constant, (lb mass/lb force)(ft/sec²);
 S resonator aperture area, ft²; m²

$$R = \frac{4}{g} \sqrt{\pi \mu \rho f} \left(\epsilon + \frac{t}{d} \right) \quad (4)$$

(ref. 3) where

- f wave frequency, 1/sec
 t resonator aperture thickness, ft; m
 d resonator aperture diameter, ft; m

ϵ nonlinear acoustic resistance parameter equal to $1 + (\Delta n l / d)$

$\Delta n l / d$ nonlinear acoustic resistance parameter from ref. 4

$$M = \frac{\rho l_{\text{eff}}}{g} \quad (5)$$

(ref. 9) where

l_{eff} effective resonator aperture thickness, ft; m

$$C = \frac{\gamma P_o S}{V} \quad (6)$$

(ref. 9) where

γ ratio of specific heats

P_o mean gas pressure, (lb force)/ft²; N/m²

V resonator cavity volume, ft³; m³

The oscillatory pressure in the cavity (based on eqs. (2) and (6)) is

$$P_{\text{int}} = \frac{C^2 P_i \sin(\omega t - \phi)}{\omega \sqrt{R_m^2 + \left(\omega M - \frac{C}{\omega}\right)^2}} \quad (7)$$

If P_{int} is maximized by picking a specific frequency and varying V , the volume corresponding to the rms value of $(P_{\text{int}}/P_i)_{\text{max}}$ is

$$V = \frac{V_o}{\beta^2 + 1} \quad (8)$$

where

V_o cavity volume for resonance, ft³; m³

β $R_m / \omega M$

The cavity volume at resonance V_o is that volume which sets

$$\frac{\left(\omega M - \frac{C}{\omega}\right)}{R_m} = 0$$

When the cavity pressure lags the incident pressure by 90° , $V = V_0$. If both the volumes for $(P_{int}/P_i)_{max}$ and V_0 are measured, β and R can be determined.

RESULTS AND DISCUSSION

Flow Profiles

Typical flow profiles measured within the wind-tunnel test section at station A-A are shown in figure 4. The flows are turbulent, with Reynold's numbers, based on test section diameter, of the order of 500 000.

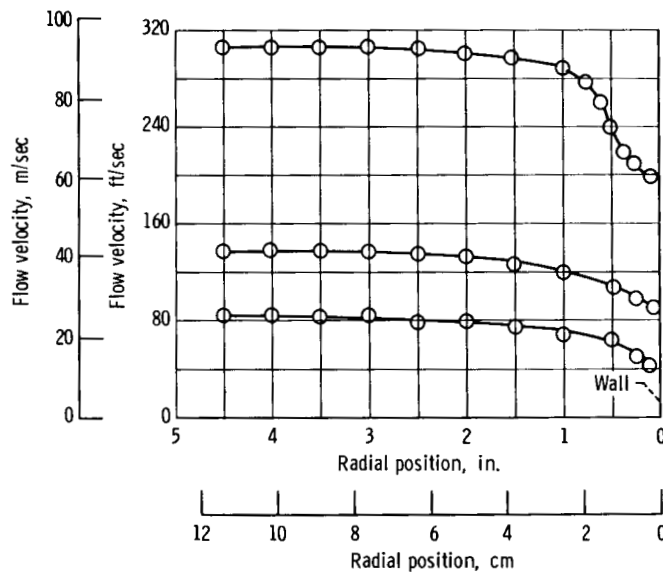


Figure 4. - Experimental flow profile.

Nonflow Evaluation

To determine the validity of the experimental procedure, a nonflow procedure was evaluated. The objective was to determine the tuning point by the phase measurement. According to reference 6, as the volume of a single resonator approaches the tuned

value, the oscillatory pressure level within the test chamber or tunnel falls to a minimum. Based on the preceding theoretical discussion, if the resonator cavity volume were varied and the chamber sound pressure level (SPL) and the phase relation of the pressures across the aperture thickness were measured, the cavity depth corresponding to tuning should be indicated by a phase angle of 90° between the pressures and a minimum in the chamber SPL. A typical result is shown in figure 5. The cavity depth of

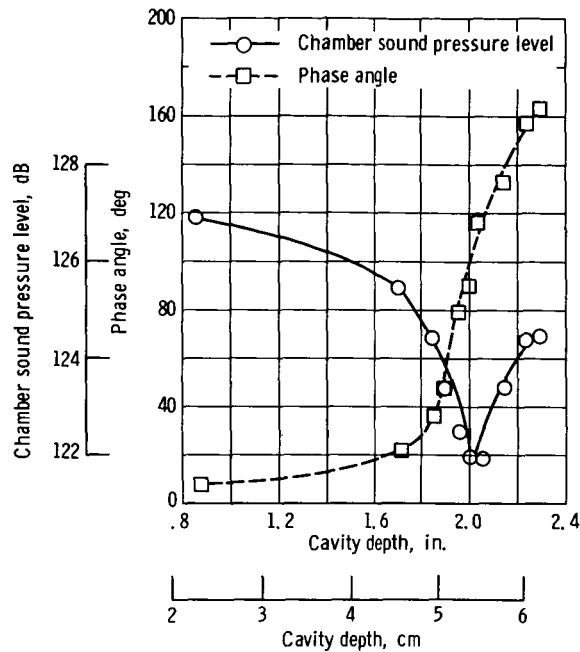


Figure 5. - Variation of phase angle and chamber sound pressure level with resonator cavity depth. Aperture diameter, 0.375 inch (0.95 cm); liner thickness, 0.1875 inch (0.475 cm); liner resonant frequency, 845 hertz; flow velocity, 0.

2 inches (5.08 cm), as indicated by the phase angle of 90° and also by the minima in SPL, corresponds to tuning. Thus, the tuned point can be determined by either measurement.

Effect of Mean Flow on Inductance as Measured by Changes in Aperture Effective Length

The effective length l_{eff} of the oscillating gas slug in a resonator aperture is equal to the mass of resonating gas in the aperture divided by the gas density and the

aperture area. The length of oscillating mass exceeds the aperture thickness. This is accounted for by the corrected aperture thickness or effective length l_{eff} . The nonflow correction factor is a function only of cavity dimensions. The equation for l_{eff} is given as

$$l_{\text{eff}} = t + \delta l_{\text{eff}}$$

$$\delta l_{\text{eff}} = 0.85 \cdot d \cdot \left(1 - 0.7 \sqrt{\frac{\pi d^2}{4A}} \right)$$

(ref. 4) where

d aperture diameter, ft; m

A resonator cavity internal cross-sectional area, ft²; m²

The effect of mean flow past the resonator aperture on the aperture effective length is presented in figure 6. The results are plotted as the ratio of the decrease in the aperture effective length $-\Delta l_{\text{eff}}$ with flow to the effective length correction factor δl_{eff}

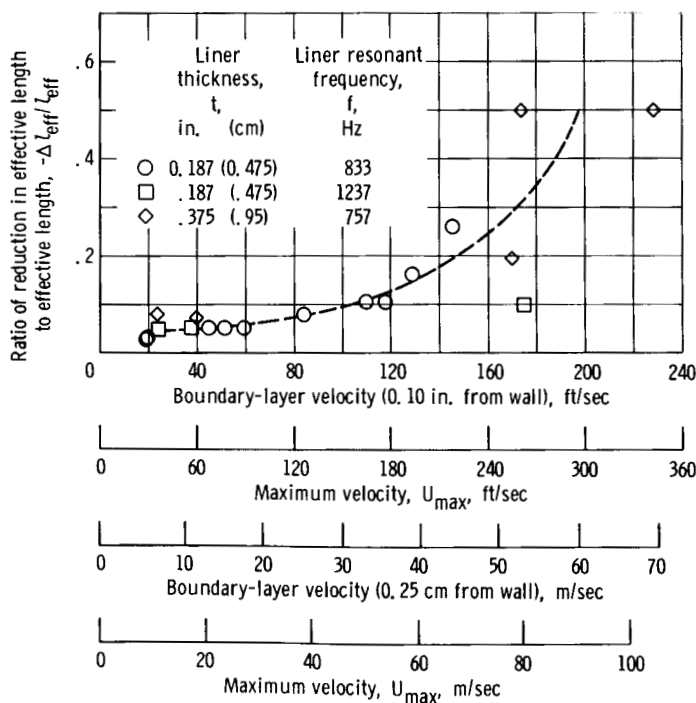


Figure 6. - Effect of mean flow on effective length. Sound pressure level, 150 decibels.

without flow. The reduction in l_{eff} is plotted as a function of the velocity measured approximately 0.1 inch (0.254 cm) from the wall. This velocity was obtained with the pitot-tube. The boundary-layer velocities are given because the turbulence in the neighborhood of the aperture must be controlled by the local rather than the free-stream velocity. The reduction in l_{eff} increased markedly at velocities greater than 80 feet per second (24.3 m/sec) up to the maximum velocity tested. The measurements were made for two aperture thicknesses at three wave frequencies. The spread of data is within the experimental error and indicates no effect of either imposed frequency or aperture thickness in the range tested. The maximum flow velocity was limited to 360 feet per second (109.8 m/sec) at the duct axis due to the decrease of signal-to-noise ratio with increasing flow velocity. The minimum signal-to-noise ratio was 10 decibels.

As to the mechanism by which the flow decreases the l_{eff} , it was suggested in reference 6 that the flow induced turbulence disrupted the laminar streamlines of the oscillatory particle motion in the neighborhood of the aperture. This would decrease the l_{eff} and increase the resonant frequency.

The effects of mean flow on the resonant frequency of a single Helmholtz resonator were also reported in reference 8. A portion of the results are shown in figure 7, a plot of cavity resonant frequency as a function of mean flow past the aperture. The measurements were made with a resonator with two orifices, the dimensions of which are given in the figure. The results show a gradual increase in resonant frequency up to a velocity of 13 feet per second (3.97 m/sec). McAuliffe attributed this increase to a decrease in the aperture mass, similar to the present experiment; however, the velocity at which no further effect was noted was considerably lower than the velocity range of the present

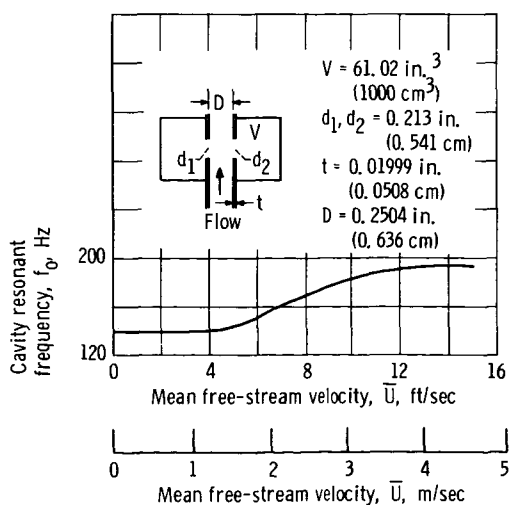


Figure 7. - Cavity resonant frequency as function of mean free-stream velocity (ref. 1, fig. 16, table III).

experiment in which no saturation or limiting value was reached. The diameter of the tube which ducted the mean flow past the resonator was 0.25 inch (0.636 cm) and no velocity profiles were given. The large differences in size of apparatus between reference 7 and the present experiment make comparison of the results questionable. It is doubted whether such results as those presented in reference 8 could be scaled to a rocket-engine environment.

Another experimental approach was the determination of the effects of mean flow on the absorption of an array of resonators (acoustic liner) reported in reference 7 and shown in figure 8. The variation in resonant frequency is caused by the decrease in λ_{eff} .

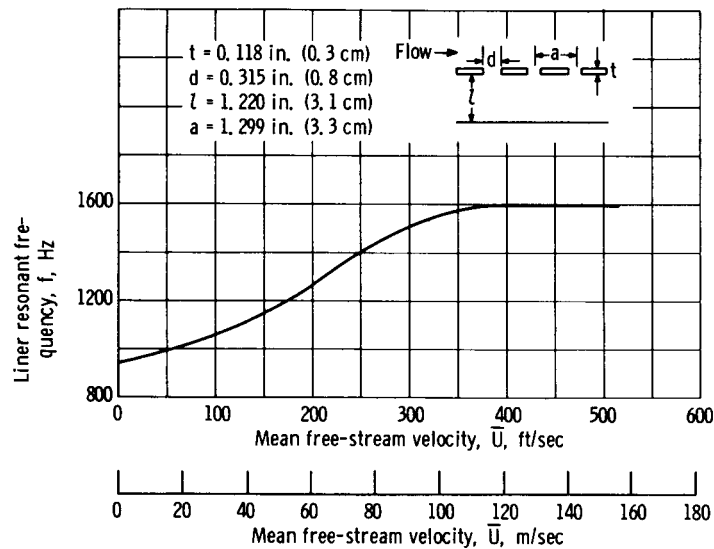


Figure 8. - Liner resonant frequency as function of free-stream velocity (ref. 6, fig. 4).

The cavity resonant frequencies are plotted as a function of the mean free-stream velocity, which was approximately 0.8 times the maximum free-stream velocity U_{max} . The liner thickness was 0.118 inch (0.3 cm) and the aperture diameter was 0.315 inch (0.8 cm). Assuming a nominal value for sonic velocity of 1100 feet per second (334 m/sec) results in values of λ_{eff} that can be calculated from the data of figure 8; these are presented in figure 9. The results indicate that the value of the λ_{eff} was reduced until there was no longer any $\delta\lambda_{eff}$ and the length of the resonant mass corresponded to the aperture thickness at a saturation velocity of approximately 350 feet per second (106.5 m/sec).

Comparison of the results of reference 7 and the present experiment is shown in figure 10. The parameter plotted is the ratio of the reduction in λ_{eff} to the λ_{eff} cor-

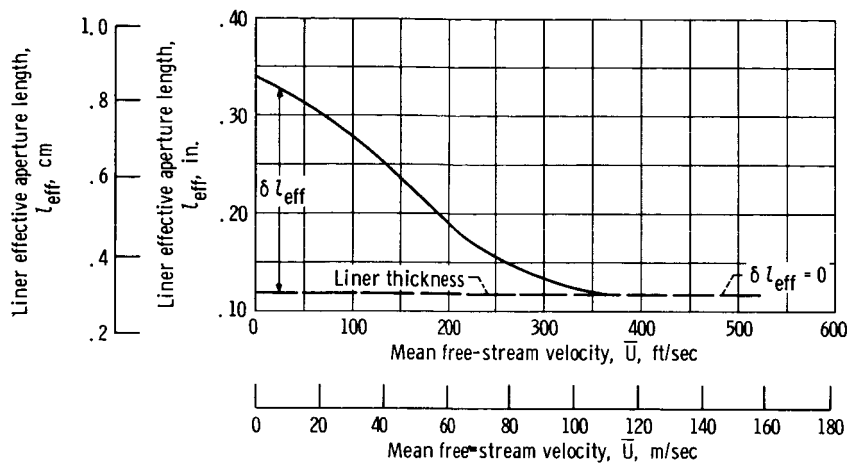


Figure 9. - Liner effective aperture length as function of mean free-stream velocity (ref. 6).

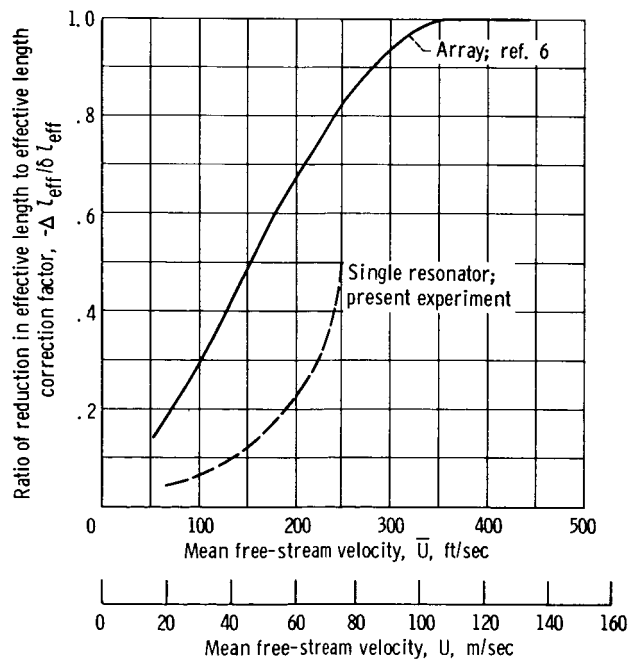


Figure 10. - Comparison of effects of mean free-stream velocity on effective length.

rection factor $(-\Delta l_{\text{eff}}/\delta l_{\text{eff}})$. When the ratio is one, the length of the resonating mass equals the aperture thickness. There is a marked difference in the results, and it is not clear which of the two is more representative of the conditions in a rocket engine. The absorber tested in reference 7 was an array of resonators, whereas the present experiment involved a single resonator. The significant flow parameter is not the mean flow but, more likely, the value of velocity or possibly turbulence near the wall. Thus, it may be that the variation between the two sets of data is due to variations in wall velocity and turbulence for the same mean velocity. Another possible explanation for this variation is the frequency-hole-spacing-flow interaction with an array liner reported in reference 6. In that investigation, certain combinations of these three parameters produced unusual behavior (absorption).

Based on the results of reference 6 and the extrapolated results of this experiment, the only tentative conclusion that may be drawn is that, in the high-flow environment typical of a rocket engine, the actual value of the aperture thickness t , rather than the corrected value $(t + \delta l_{\text{eff}})$, should be used for an aperture effective length.

Effect of Mean Flow on Acoustic Resistance

The effects of mean flow on the aperture acoustic resistance, as presently used in the design scheme of reference 2, are based on flow past a woven mesh screen. To have a more realistic set of results with which to compare the data of the present experiment, it is necessary to examine other results of reference 7. In figure 4 of reference 7, plots of absorption as a function of frequency for various flow velocities are given. By a simple electrical analogy, it can be demonstrated that the acoustic resistance of the array is equal to the product of the reactive mass and the bandwidth of the absorption peaks at half the maximum absorption. If this product is normalized with respect to its value at the no flow condition, a measure of the effect of flow on the resistance can be obtained. These results are shown as circular symbols in figure 11.

The results of the present experiment, as indicated by the square symbols in figure 11 are in approximate agreement with those of reference 7. A quiescent region where no flow effects are seen is terminated by a threshold velocity at 150 to 200 feet per second (45.8 to 61 m/sec) at which point a linear increase in resistance with flow is seen. It can be seen that mean flow can increase the aperture resistance by a factor of 4 in the range shown. It is recommended that the dashed line of figure 11, representing an average result, be used for predicting the effects of mean flow on resistance for the design of an acoustic liner.

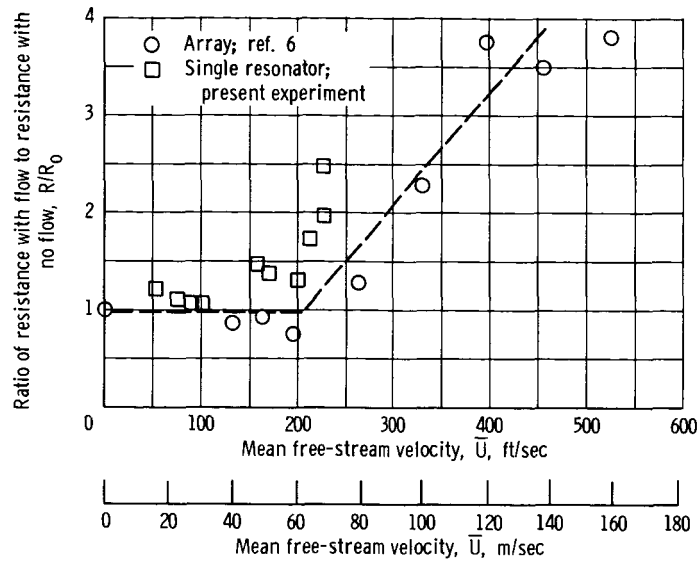


Figure 11. - Effect of mean flow on acoustic resistance. (Circular symbols based on the assumption $R = \rho_0(l_{eff}/g_c)2\pi\Delta f$.)

Effect of High-Wave Amplitude on Acoustic Resistance

The effect of wave amplitude on the resonator acoustic resistance is presented in figure 12. The acoustic resistance R as indicated by equation (4) in the THEORY section of this report, is equal to some function of the frequency and gas properties multi-

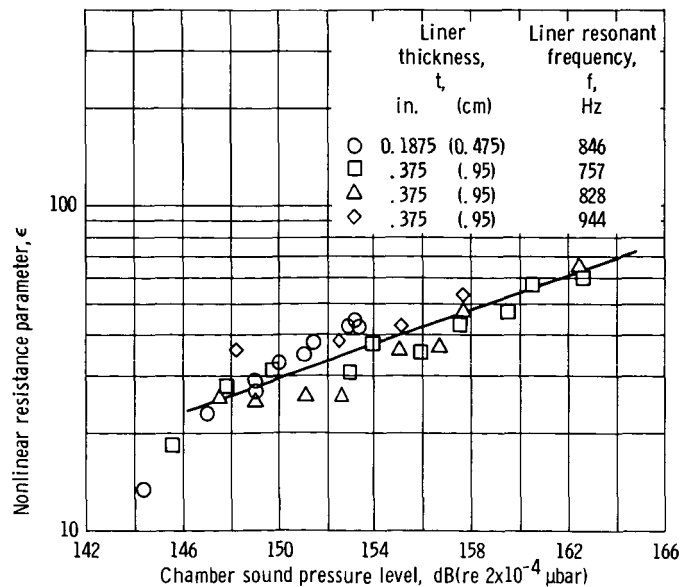


Figure 12. - Effect of chamber sound pressure level on nonlinear resistance parameter.

plied by the term $(\epsilon + t/d)$ where t/d represents the frictional loss and ϵ represents an empirical correction for high-wave amplitude effects. For high-wave amplitudes, ϵ becomes the more important term in the equation. By experimentally determining the resistance, ϵ can be determined using equations (3) and (4). Figure 12 is a plot of ϵ as a function of the wave amplitude.

Measurements were made for two thicknesses and four frequencies. The variation due to changes in thickness or frequency is within experimental error and, consequently, no effect of frequency or thickness is perceivable over the range of variables studied. The results are compared with similar results from references 2 to 5 in figure 13, and there seems to be reasonable agreement with the results of reference 5.

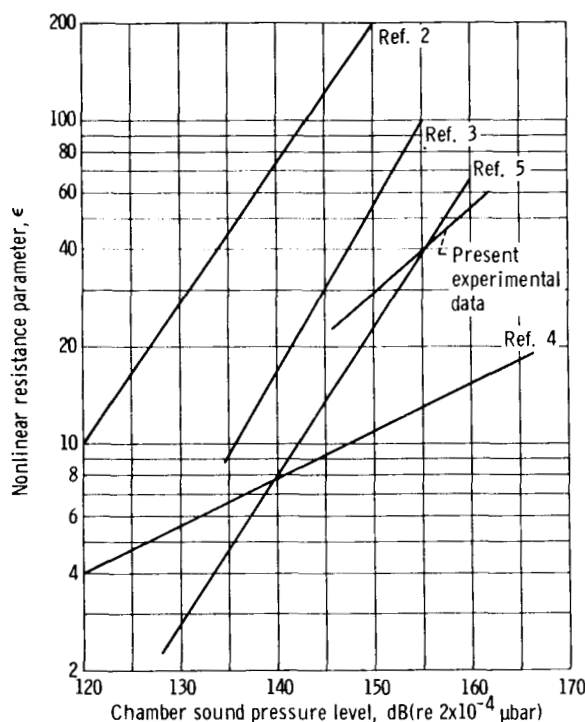


Figure 13. - Nonlinear resistance parameter as function of chamber sound pressure level.

Another approach to the effect of high-wave amplitude on the acoustic resistance is described in references 8 and 10. The acoustic resistance is attributed to a jet expansion loss at the exit of the aperture. The functional form of the loss should be more closely related to a simple pressure drop due to flow ($\Delta P_{g_c}/v' = \rho v' = \text{resistance}$, where v' is the acoustic particle velocity) than to an empirical correction ϵ to a linear viscous loss. The acoustic-resistance data are plotted in figure 14 with a line representing $R = \rho v'$. The data cluster closely around the line, which indicates that the acoustic re-

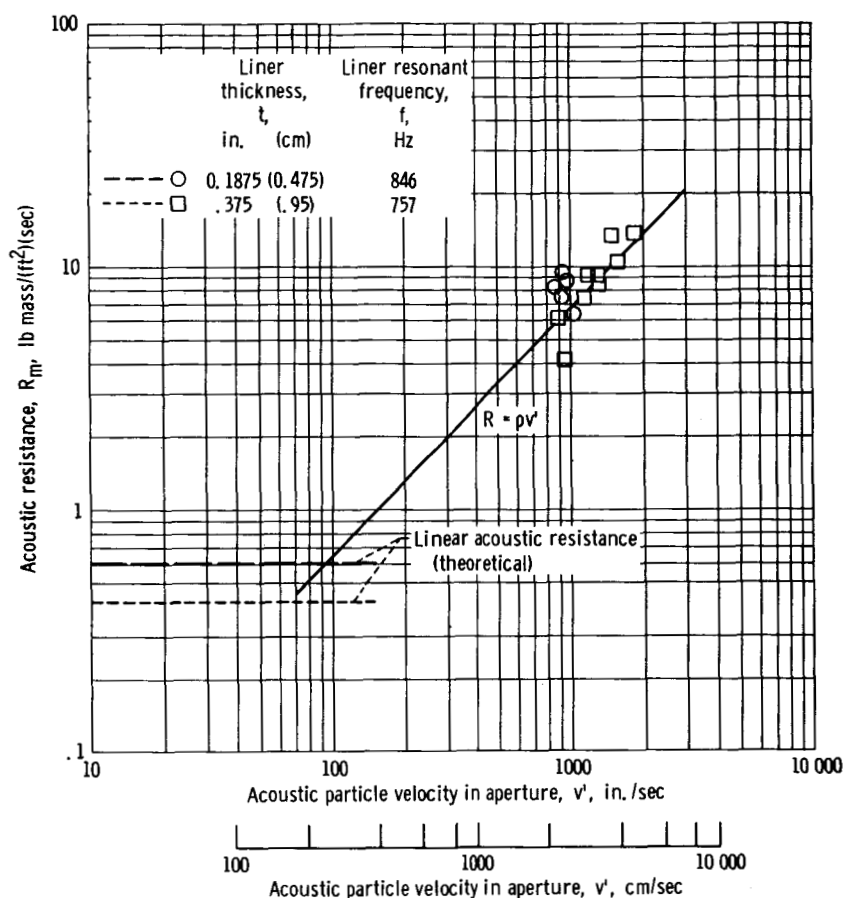


Figure 14. - Acoustic resistance as function of acoustic particle velocity.

sistance at high-particle velocities is simply the jet loss without any friction (linear) effects (The frictional effects are obtained from eq. (4) in the THEORY section by setting $\epsilon = 1$). Presented on the same plot are the linear acoustic resistances for the two frequencies, with transition at $v' = 60$ to 90 inches per second (152.3 to 228 cm/sec). The transition velocity corresponds to the velocity $v' = R_{\text{linear}}(\epsilon = 1)/\rho$. At that velocity, the nonlinear jet losses begin to have an effect. At the same time, turbulence in the neck should destroy the laminar oscillatory flow and change or eliminate the character of the linear velocity losses. A Reynolds number based on the acoustic particle velocity is 900 to 1800 which approximates the standard transition Reynolds number of 2100 . Consequently, the transition from linear to nonlinear resistance seems to be similar to the transition to turbulence in pipe flow.

SUMMARY OF RESULTS

1. Based on the magnitude of the mean flows and turbulence in a rocket combustor, it is suggested that the length of the resonating mass be considered equal to the aperture or liner thickness.

2. The effect of mean flow past the resonator apertures is to raise the acoustic resistance by up to a factor of 4 in the flow range evaluated.

3. The effect of high-wave amplitude on the acoustic resistances can be explained by a jet loss so that the acoustic resistance is equal to $\rho v'$ where v' is the acoustic particle velocity. The transition in the effects of mean flow and high-wave amplitude may be related by a turbulent transition mechanism in the aperture.

Lewis Research Center,

National Aeronautics and Space Administration,

Cleveland, Ohio, February 15, 1968,

128-31-06-05-22.

REFERENCES

1. Wanhainen, John P.; Bloomer, Harry E.; Vincent, David W.; and Curley, Jerome K.: Experimental Investigation of Acoustic Liners to Suppress Screech in Hydrogen-Oxygen Rockets. NASA TN D-3822, 1967.
2. Alexander, George: Acoustic Liner Damps Rocket Combustion Instability. Aviation Week & Space Tech., vol. 83, no. 6, Aug. 9, 1965, pp. 72-79.
3. Ingard, Uno: On the Theory and Design of Acoustic Resonators. J. Acoust. Soc. Am., vol. 25, no. 6, Nov. 1953, pp. 1037-1061.
4. Blackman, A. W.: Effect of Nonlinear Losses on the Design of Absorbers for Combustion Instabilities. ARS J., vol. 30, no. 11, Nov. 1960, pp. 1022-1028.
5. Marino, P. A., Jr.; Bohn, N.; and Garrison, G. D.: Measurement of Acoustic Resistance at Sound-Pressure Levels to 171 dB. J. Acoust. Soc. Am., vol. 41, no. 5, May 1967, pp. 1325-1327.
6. Phillips, Bert; and Morgan, C. Joe: Mechanical Absorption of Acoustic Oscillations in Simulated Rocket Combustion Chambers. NASA TN-3792, 1967.
7. Mechel, F.; Mertens, P.; and Schilz, W.: Research on Sound Propagation in Sound-Absorbent Ducts with Superimposed Air Streams. Final Rep. (AMRL-TDR-62-140, vols. II and III), Physikalisches Inst., Univ. Göttingen, West Germany, Dec. 1962.

8. McAuliffe, Clinton E.: The Influence of High-Speed Air Flow on the Behavior of Acoustical Elements. M. Sc. Thesis, Mass. Inst. Tech., 1950.
9. Zwikker, C.; and Kosten, C. W.: Sound Absorbing Materials. Elsevier Publishing Co., Inc., 1949.
10. Harrje, David T.; and Sirignano, William A.: Nonlinear Aspects of Combustion Instability in Liquid Propellant Rocket Motors. Rep. No. 553F (NASA CR-77672), Princeton Univ., June 1, 1966, p. 38.